chemosensors

MDPI

Article

Potentiometric Surfactant Sensor for Anionic Surfactants Based on 1,3-dioctadecyl-1*H*-imidazol-3-ium tetraphenylborate

Nikola Sakač [1,*], Dubravka Madunić-Čačić [1,2], Dean Marković [3], Lucija Hok [4], Robert Vianello [4], Valerije Vrček [5], Bojan Šarkanj [6], Bojan Đurin [7], Bartolomeo Della Ventura [8], Raffaele Velotta [8] and Marija Jozanović [9,*]

1 Faculty of Geotechnical Engineering, University of Zagreb, 42000 Varaždin, Croatia
2 Saponia Chemical, Pharmaceutical and Foodstuff Industry, Inc., 31000 Osijek, Croatia
3 Department of Biotechnology, University of Rijeka, 51000 Rijeka, Croatia
4 Laboratory for the Computational Design and Synthesis of Functional Materials, Division of Organic Chemistry and Biochemistry, Ruđer Bošković Institute, 10000 Zagreb, Croatia
5 Department of Organic Chemistry, Faculty of Pharmacy and Biochemistry, University of Zagreb, A. Kovačića 1, 10000 Zagreb, Croatia
6 Department of Food Technology, University North, 48000 Koprivnica, Croatia
7 Department of Civil Engineering, University North, 42000 Varaždin, Croatia
8 Department of Physics "E. Pancini"—Università Di Napoli Federico II, 80126 Napoli, Italy
9 Department of Chemistry, University of Osijek, 31000 Osijek, Croatia
* Correspondence: nikola.sakac@gfv.unizg.hr (N.S.); mjozanovic@kemija.unios.hr (M.J.); Tel.: +385-915830336 (N.S.); +385-996865716 (M.J.)

check for updates

Citation: Sakač, N.; Madunić-Čačić, D.; Marković, D.; Hok, L.; Vianello, R.; Vrček, V.; Šarkanj, B.; Đurin, B.; Della Ventura, B.; Velotta, R.; et al. Potentiometric Surfactant Sensor for Anionic Surfactants Based on 1,3-dioctadecyl-1*H*-imidazol-3-ium tetraphenylborate. *Chemosensors* **2022**, *10*, 523. https://doi.org/10.3390/chemosensors10120523

Academic Editors: Iulia Gabriela David and Dana Elena Popa

Received: 14 November 2022
Accepted: 7 December 2022
Published: 8 December 2022

Publisher's Note: MDPI stays neutral with regard to jurisdictional claims in published maps and institutional affiliations.

Copyright: © 2022 by the authors. Licensee MDPI, Basel, Switzerland. This article is an open access article distributed under the terms and conditions of the Creative Commons Attribution (CC BY) license (https://creativecommons.org/licenses/by/4.0/).

Abstract: As anionic surfactants are used as cleaning agents, they pose an environmental and health threat. A novel potentiometric sensor for anionic surfactants based on the 1,3-dioctadecyl-1*H*-imidazol-3-ium tetraphenylborate (DODI–TPB) ionophore is presented. The newly developed approach for DODI–TPB synthesis is faster and simpler than the currently used strategies and follows the green chemistry principles. The DODI–TPB ionophore was characterized by computational and instrumental techniques (NMR, LC–MS, FTIR, elemental analysis) and used to produce a PVC-based DODI–TPB sensor. The sensor showed linear response to dodecylbenzenesulfonate and dodecyl sulfate in concentration ranges of 6.3×10^{-7}–3.2×10^{-4} M and 5.9×10^{-7}–4.1×10^{-3} M, for DBS and SDS, respectively. The sensor exhibits a Nernstian slope (59.3 mV/decade and 58.3 mV/decade for DBS and SDS, respectively) and low detection limits (7.1×10^{-7} M and 6.8×10^{-7} M for DBS and SDS, respectively). The DODI–TPB sensor was successfully tested on real samples of commercial detergents and the results are in agreement with the referent methods. A computational analysis underlined the importance of long alkyl chains in $DODI^+$ and their C–H···π interactions with TPB^- for the ionophore formation in solution, thereby providing guidelines for the future design of efficient potentiometric sensors.

Keywords: anionic surfactants; computational analysis; green chemistry; quaternary ammonium compounds; synthetic ionophore; potentiometric sensor

1. Introduction

Surfactants are organic molecules which decrease the tension of the surface. Their structure usually consists of a hydrophilic and a hydrophobic part. Depending on the charge, surfactants are grouped into anionic, cationic, amphoteric, and nonionic (with no charge). Surfactants can be classified as zwitterionics, depending on their charge. Cationic surfactants are used as disinfecting agents and as preservatives [1,2], while anionic surfactants are used for cleaning and washing [3]. Nonionic surfactants are employed for enhancing surfactant activity, reducing foaming, and enhancing cleaning. Anionic surfactants participate in 70% of the global surfactant market, which is expected to increase by 4.5% in the period from 2020 to 2025 due to high demand and standard growth [4].

Anionic surfactants are used in many products of daily life and in the industry sector (recently for electric vehicles [5]), which is why they are also likely to be found in wastewater, rivers, and lakes. Apart from the foaming effect, the negative consequences on the environment include their aptitude to prevent oxygen and gas exchange at the water surface; moreover, they easily degrade the cell membrane—as they have a similar nature to lyophilic molecules in the phospholipid bilayer of the cell, cause skin irritation, etc. [6,7]. Cationic surfactants are the most toxic, compared to the other types of surfactants.

Anionic surfactants in water are usually quantified by highly manual procedures, such as methylene blue active substances (MBASs), two-phase titration [8], or instrumental methods, such as liquid chromatography and gas chromatography [3]. These manual procedures are time-consuming, slow, low in reproducibility, and require specialized personnel, while instrumental methods are faster, but need expert personnel, toxic solvents, and expensive instrumentation, as well as they can often be performed only in confined spaces.

Compared to the above analytical procedures, the ion-selective electrodes (ISEs) for the surfactants are robust, simple, fast, and do not use toxic solvents. They can also be portable and used in field measurements [9]. In addition, ISEs are not affected by color changes or transparency problems. ISEs are also capable of measuring concentrations of anions and cations, depending on which ionophore is used [10–14]. All the above advantages are used to fabricate surfactant sensors for measuring cationic surfactants, nonionic surfactants, and anionic surfactants in aqueous media [1,15]. There are mainly two types of surfactant sensors: solid-state surfactant sensors [16,17] and PVC-based liquid membrane-type surfactant sensors [18]. Membranes based on PVC consist of a high molecular weight PVC and a plasticizer in a 2:1 weight ratio, and usually a 1% ionophore, which is an active substance of the sensing membrane [19]. The plasticizer softens the PVC and serves as a solvent for the highly lipophilic ionophore. Ionophores are poorly soluble and possess high molecular weight, associates (ion-pairs) of the cationic surfactant and anionic surfactant, or some high lipophilic counter ions. The role of the ionophore, as a sensing element, is mainly determined by its potential and ability to handle complex interactions with the analyte in its binding sites [20]. Synthetic ionophores designed according to their complexation constants can provide improved electrochemical ionophores leading to the development of optimized sensors with higher selectivity, reproducibility, and longer sensor lifetime [21]. Different commercially available quaternary ammonium compounds (QACs) have been used as a part of the ionophores for anionic surfactants detection, namely dodecyltrimethylammonium [22], cetyltrimethylammonium [23], hyamine [24], 1,3-dihexadecyl-1*H*-benzo[*d*]imidazol-3-ium recently described by our group [1], and others. The introduction of a designed QAC for potentiometric sensor provides a sensing material with planned and improved properties compared to classical ion exchangers.

The aim of this work is to present a new strategy for the direct synthesis of a new ionophore, namely 1,3-dioctadecyl-1*H*-imidazol-3-ium tetraphenylborate (DODI–TPB), and to use it as a sensing component in the preparation of a new DODI–TPB-based surfactant sensor for the quantification of anionic surfactants by potentiometric titrations in real samples of commercial products. The ionophore was extensively studied by computational and instrumental techniques such as NMR, LC–MS, FTIR-ATR, and elemental analysis. The fabricated DODI–TPB surfactant sensor was characterized analytically in terms of response, pH influence, selectivity, and accuracy.

2. Materials and Methods

2.1. Reagents

Chemical reagents used for organic synthesis were all analytical grade chemicals: 1-bromooctadecane, 1*H*-imidazole, and $NaHCO_3$ (Sigma Aldrich, Darmstadt, Germany) and utilized without further purification.

For measurements of the direct potentiometric response of anionic surfactant, analytical grade sodium dodecylsulfate (SDS) and technical grade sodium dodecylbenzenesulfonate (DBS) (all from Fluka, Buchs, Switzerland) were used. Titrations were performed

using benzethonium chloride (Hyamine 1622), hexadecyltrimethylammonium bromide (CTAB), cetylpyridinium chloride (CPC), and 1,3-didecyl-2-methylimidazolium chloride (DMIC) (all analytical grade from Merck, Munich, Germany). Ultrapure deionized water was used for all measurements.

For sensing membrane preparation, a high molecular weight PVC and an analytical grade plasticizer *o*-nitrophenyloctylether (*o*-NPOE) (both from Sigma Aldrich, Darmstadt, Germany) were used. The solvent was tetrahydrofuran (THF) (Merck, Munich, Germany).

For interference measurements a series of organic and inorganic anions were used; acetate, borate, benzoate, bromide, chloride, carbonate, dihydrogenphosphate, EDTA, hydrogen sulfate, nitrate, sulfate, all analytical grade sodium salts (all from Kemika, Zagreb, Croatia).

2.2. Ionophore Synthesis and Characterization

Bisalkylated imidazole product (1) was synthesized according to the literature's procedure with some modifications. Alkylation reaction was conducted by adding 0.25 g 1*H*-imidazole (3.37 mmol) and 200 mg $NaHCO_3$ (2.38 mmol) in anhydrous acetonitrile (10 mL) and stirring at 90 °C for 1 h. Then, the solution was cooled and 5 g 1-bromooctadecane (15.00 mmol) was slowly added to the mixture and continued to be vigorously stirred at 120 °C under an inert nitrogen atmosphere for 48 h. The product was washed with methanol and hexane three times. Flash column purification was conducted in DCM/methanol = 10:0.25. The product was dried under a vacuum at 40 °C for 4 h. The desired product (1) (2.00 g, 3.06 mmol) was obtained in a 90.75% yield.

To prepare the sensing ion-pair DODI–TPB, 1.50 g (2.29 mmol) of 1,3-dioctadecyl-1*H*-imidazol-3-ium bromide (1) was mixed for 6 h with 1.50 g (4.38 mmol) of sodium tetraphenylborate, in 100 mL of acetonitrile. This mixture was filtered, washed with dichloromethane, cooled in a freezer for 24 h, and then again filtered. Dichloromethane was removed by rotary evaporation for 3 h. A total of 3.39 g (mmol) of DODI–TPB ionophore was produced as a white solid (yield: 86.44%). After the evaporation of dichloromethane, the crude DODI–TPB (2) was dried at 80 °C to the constant mass. Such prepared ion-pair was used for sensor membrane fabrication.

The DODI–TPB ion-pair was analyzed by FTIR–ATR spectrometer Spectrum Two (Perkin Elmer, Waltham, MA, USA).

The ^{1}H NMR spectra were recorded at 400 MHz and ^{13}C NMR spectra at 100.613 MHz by a VARIAN INOVA 400 (Varian, Crawley, United Kingdom).

MS spectra were recorded in q1 ms scan mode at API 2000 LC-ESI-MS/MS (Applied Biosystems, Foster City, CA, USA).

PerkinElmer 2400 CHNS/O Series II System was used for the elemental analysis (PerkinElmer Inc., Waltham, MA, USA).

2.3. Computational Details

RESP charges at the HF/6–31G(d) level were used to describe the DODI-cation, while the TPB^{-} anion was parameterized in line with the literature's recommendations. [25] Both ions were positioned in a 15 Å rectangular box and solvated with 8.553 water molecules and supplemented with Na^{+} and Br^{-} counterions to assure electrical neutrality. Such a system underwent the geometry optimization in AMBER 16 [26] with periodic boundary conditions in all directions, followed by a 30 ps equilibration under NTV conditions and a gradual temperature increase from 0 to 300 K. This was, then, submitted to 300 ns of productive and unconstrained MD simulations, with a time step of 2 fs at a constant pressure of 1 atm and temperature of 300 K, employing a threshold of 11.0 Å to truncate the nonbonded interactions. The binding energies between sensor components, ΔG_{BIND}, were obtained through the MM-PBSA analysis [27,28], in line with our recent reports on similar systems [29–31], utilizing every second snapshot, 75.000 in total, recorded from the entire MD trajectory.

2.4. Preparation of Surfactant SENSOR

The surfactant sensor membrane was prepared by dissolving a high molecular weight PVC in a plasticizer *o*-NPOE (1:2) by sonication. Then, 1% of the ion-pair was added. Next, 2 mL of THF was added and sonicated for 15 minutes. After this, the cocktail was poured into the glass mold and left to dry for 1 day. The membrane was planted at the bottom of the Philips electrode body IS-561 (Supelco, Bellefonte, PA, USA). NaCl (3 M) was used as an inner electrolyte.

2.5. Potentiometric Measurements

Surfactant sensor characterizations of the DODI–TPB surfactant sensor by direct potentiometry were performed by Metrohm 794 Basic Titrino with a stirred paired with Metrohm 781 pH meter (Metrohm, Herisau, Switzerland) and a reference electrode silver/silver (I) chloride electrode with potassium chloride (3 M) electrolyte (Metrohm, Herisau, Switzerland). To obtain the response characteristics, selected cationic surfactants (Hyamine 1622, CPC, CTAB, and DMIC) were incrementally added to the deionized water to reach a concentration range from 1×10^{-8} to 1×10^{-2} M. Response time was set to 90 seconds. An interference study was performed on selected organic and inorganic anions usually found in commercial product formulations or in wastewaters. Solution of interfering anion (0.01 M) was placed in a beaker and CPC was incrementally added (0.5 mM) and measured in 90 seconds intervals. IUPAC fixed interference method was used to calculate the potentiometric selectivity coefficients. The effect of pH change was observed for CPC (0.5 mM) at pH levels from 2 to 12.

Potentiometric titrations were performed by Metrohm 808 Titrando with a stirrer, a reference electrode silver/silver (I) chloride electrode with potassium chloride (3 M) electrolyte, and a Metrohm Tiamo software (all from Metrohm, Herisau, Switzerland). SDS (0.4 mM) and DBS (0.4 mM) were titrated with the corresponding concentration of the selected cationic surfactants Hyamine 1622, CTAB, CPC or DMIC, and a DODI–TPB surfactant sensor as an endpoint indicator. The anionic surfactant contents in 12 commercial products were measured by potentiometric titration with CPC in corresponding concentrations and a DODI–TPB surfactant sensor as an endpoint indicator.

3. Results

3.1. Ionophore Synthesis and Characterization

A new, faster, and simpler way for the direct synthesis of ion-pairs was presented (Scheme 1). The common synthesis of ion-pairs employs anionic and cationic surfactants, or large lipophilic ions [32,33]. In the presented approach, the preparation of the ion-pair was achieved by the direct addition of the counter ion (TPB) into the reaction mixture containing the newly synthesized cationic surfactant. The latter two-steps one-pot process is much faster, simpler, and employs less toxic chemicals, which is consistent with the green chemistry principles. A detailed characterization of DODI-Br by MS, ^{1}H NMR, and ^{13}C NMR spectroscopy and elementary analysis and the detailed data is offered in the supplementary materials (Figures S1–S3). The C2 symmetry of DODI-Br and DODI–TPB simplified their NMR spectra. As seen from the ^{1}H NMR spectrum of DODI-Br, the newly formed triplets of methylene signals of -CH_2N = arrived at 4.37 ppm, while the other methylene signals of alkyl chains range from 1.95 to 1.25 ppm. The ^{1}H NMR signals of ^{1}H-imidazole were identified at 10.57 and 7.41 ppm. The characteristic signal of -CH_2N = in the ^{13}C NMR spectrum arrived at 50.1 ppm. The other carbons of the methylene chain groups appeared between 31.9 and 22.7 ppm. The signals at 137.3 and 121.8 can be attributed to the ^{1}H-imidazole unit. In the IR spectrum C = N, C-N stretching was assigned as strong adsorptions at 1650 and 1150 cm^{-1}. The presence of bromine was confirmed by MS and elemental analysis.

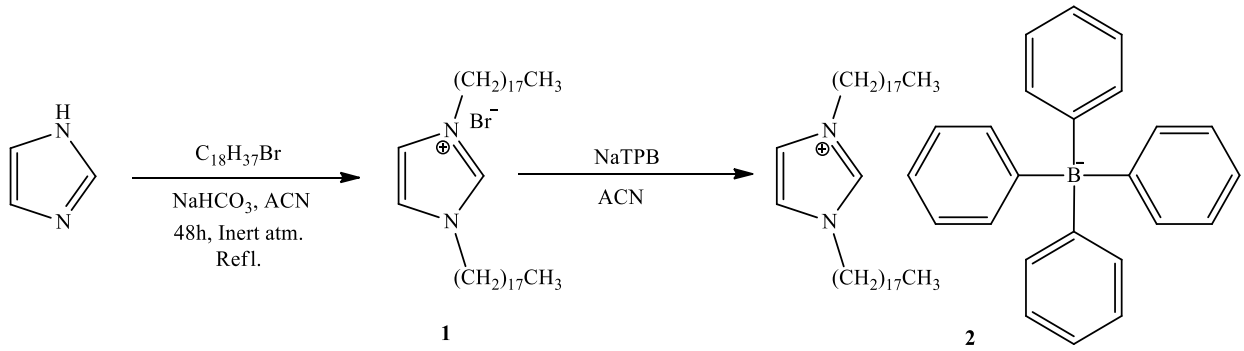

Scheme 1. Synthesis of DODI–TPB ion-pair sensing complex (2) via quaternary alkyl ammonium salt 1,3-dioctadecyl-1*H*-imidazol-3-ium bromide (1).

Characterization of DODI–TPB was also performed. Its ^{1}H NMR spectrum confirmed the presence of the TPB anion. The phenyl -CH = signals were identified in the range of 7.57–7.46 and at 7.00 and 6.83 ppm. Other ^{1}H NMR signals were also consistent with the proposed DODI–TPB structure. Due to the carbon–boron coupling in the ^{13}C NMR spectrum, the signal at 164.0 ppm was a quartet, while the other C atoms of TPB and ^{1}H imidazole were identified at 135.9, 134.9, 125.9, 121.9, and 120.7. ^{13}C-signals of alkyl chains appeared at 49.4, 31.9, and in the range between 29.8 and 14.1 ppm. Similar to DODI-Br, DODI–TPB showed the IR-stretching of C = N, C-N at 1650 and 1150 cm^{-1}. The MS spectrum and elemental analysis were also consistent with the proposed DODI–TPB structure.

3.2. Computational Analysis

Computational analysis was employed to inspect the dynamics and features of the investigated DODI^{+} cation in the water solution and elucidate intermolecular interactions responsible for its complexation with TPB^{-}. We mainly focused on characterizing the DODI–TPB adduct through electronic, geometric, and thermodynamic features.

Despite containing a rigid imidazole skeleton, DODI^{+} has two unconstrained C-18 chains, whose flexibility over the anionic TPB^{-} is clearly evident in the obtained RMSD plots (Figure S4). Interestingly, it appears that it is precisely this feature of DODI^{+} that is essential for its effective TPB^{-} recognition through a range of favorable C–H$\cdots\pi$ interactions with the aromatic phenyl rings in the latter.

DODI–TPB complexation is a favorable, yet reversible, event, due to the adduct formation and its dissociation exchange during the MD simulation. To illustrate that, the matching distance graphs reveal that the relevant N(DODI^{+})$\cdots$B(TPB^{-}) distances extend much beyond 40 Å, while taking values below 12 Å in around 48% of the recorded structures (Figure S5). Since DODI^{+} is not a globular molecule, we identified the latter as the upper limit beyond which no appreciable interactions were observed. In order to quantify these interactions, the calculated MM-PBSA binding free energy shows that the DODI–TPB complex formation is indeed exergonic at $\Delta G_{BIND} = -5.0$ kcal mol^{-1}, which confirms its feasibility (Table 1). To put the latter number in an appropriate context, and given the highly favorable sensing features of the DODI–TPB system, let us mention that precisely the same ΔG_{BIND} value was obtained for the benzimidazole analogue of DODI^{+} with a slightly shorter C-16 alkyl chain. [29] This indicates that the calculated ΔG_{BIND} value falls into an optimal range as it needs to ensure two opposing aspects, namely the stability of the adduct and the reversibility of its formation, the latter being essential for its sensing features through the potential exchange with other anionic analytes.

Table 1. MM-PBSA calculated binding affinities (ΔG_{BIND}, in kcal mol^{-1}) among the TPB^- anion and selected cations following the molecular dynamics simulation in water.

Cation Component	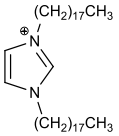	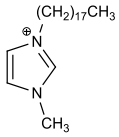	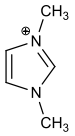	$CH_3(CH_2)_{34}CH_3$
ΔG_{BIND}	−5.0	−2.4	−0.5	−3.2

The representative adduct structure (Figure 1) shows three kinds of favorable interactions, namely (i) the π···π stacking contacts among charged imidazole in $DODI^+$ and a phenyl ring in TPB^-, (ii) the C–H···π interactions involving the central imidazole carbon and the other phenyl ring in TPB^-, and (iii) a range of C–H···π interactions that both C-18 chains form with the remaining phenyl groups in TPB^-. Interestingly, in the elucidated structure, the matching B(TPB^-)···N($DODI^+$) distances are 5.4 and 5.7 Å, which is in excellent agreement with the calculated RDF plot, which indicates the largest number of these contacts assuming values around 5.7 Å (Figure 1), and therefore validating the identified structure as representative.

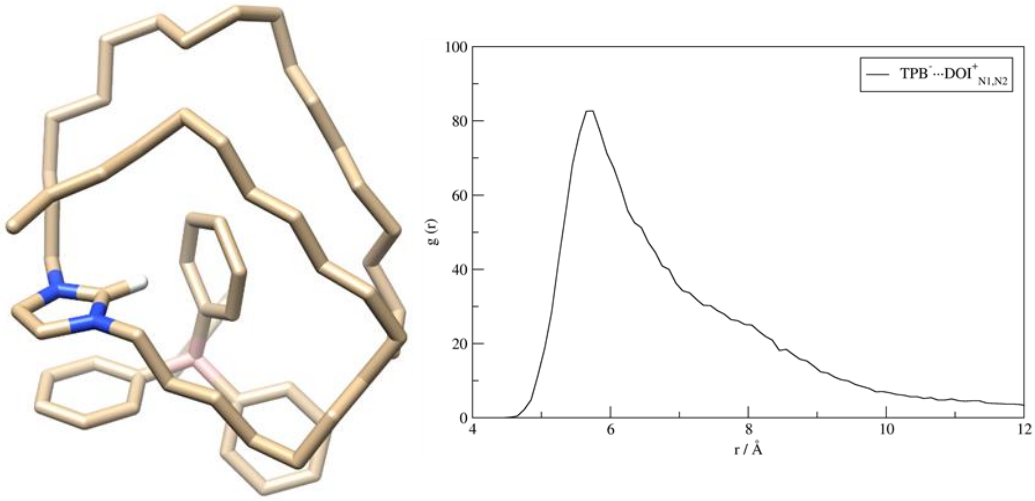

Figure 1. Representative structure of the DODI–TPB complex in the aqueous solution ((**left**); hydrogen atoms omitted for the clarity) as elucidated from the 300 ns molecular dynamics simulation, and the matching RDF graph considering N($DODI^+$)···B(TPB^-) distances with the peak value located at 5.7 Å (**right**).

Such vicinity between boron and nitrogen atoms could lead to the assumption that the electrostatic attraction determines the binding among components. Yet, this can be excluded as it follows from the analysis of atomic charges prior and after the adduct formation (Figure S6). The results show that, before binding, the imidazole unit in $DODI^+$ accommodates only one-third of the excess positive charge (0.33 |e|), while the rest is accumulated within its C-18 chains, which is, interestingly, not changed in the formed adduct. In fact, once DODI–TPB is formed, only 2% of the total charge density is exchanged between components, as is evident in the sum of all atomic charges on $DODI^+$ and TPB^- being +1.02 and −0.98 |e|, respectively, which eliminates electrostatic interactions as predominantly responsible for the adduct stability.

In addition, the extent of the π···π stacking interactions was estimated by analyzing distances between the center of mass of the imidazole ring in $DODI^+$ and that of each phenyl group in TPB^-. Adopting the value of 4 Å as the recommended threshold for these contacts [29], it resulted that these interactions take place in only 2.2% of structures occurring during MD simulations. Along these lines, the frequency of the C–H···π interactions

involving the central imidazole C–H group was analogously inspected and we counted 5.7% of structures where this was identified. Therefore, both sets of values suggest only a very limiting significance of both of these interactions for the complex formation.

Lastly, due to a large number of C–H groups within both C-18 chains potentially engaging in the C–H···π interactions with TPB^-, in evaluating their frequency we have repeated the MD simulations with several model cationic components, having either one or both C-18 chains replaced by a methyl group (Table 1). The results show that when one of the C-18 chains is already substituted by a smaller methyl unit, the binding affinity is reduced in half ($\Delta G_{BIND} = -2.4$ kcal mol^{-1}), while it exhibits an even larger further decrease when no C-18 chains are present ($\Delta G_{BIND} = -0.5$ kcal mol^{-1}). This evidently underlines the crucial effect of the long alkyl chains and highlights this type of interaction as dominant in recognizing and binding the TPB^- in solution. Such a conclusion is further supported by analyzing the situation with a simple alkane, with its length, C-36, equaling the sum of both chains in $DODI^+$. Interestingly, despite being formally uncharged, the affinity of $C_{36}H_{74}$ towards TPB^- surpasses those from both model cationic imidazoles and achieves $\Delta G_{BIND} = -3.2$ kcal mol^{-1} (Table 1), thereby reaching 64% of the affinity of the full $DODI^+$. We believe all of this clearly illustrates the importance of these hydrophobic fragments and their flexibility for the efficient TPB^- binding, and it provides useful guidelines for the future design of efficient potentiometric sensors based on selected ionophores.

3.3. Sensor Characterization

3.3.1. Sensor Response to Anionic Surfactants

According to the modified Nernst equation, the electromotive force of the surfactant sensor membrane in the presence of anionic surfactant is the following:

$$E = E^0 - Sloga_{AS^-}$$

where E^0 is a constant potential term, S is a slope in the linear part of the response curve, and a_{AS^-} is an activity of the investigated surfactant anion.

The first step in DODI–TPB surfactant sensor characterization was to observe the direct potentiometric response of the sensor for two anionic surfactants, namely DBS and SDS, over a wide range of concentrations in deionized water. In this way, it is possible to determine the response of the sensor for the desired anions. The response curves and response characteristics for DBS and SDS are presented in Figure 2 and Table 2. For the DBS anion, the linear concentration range was from 6.3×10^{-7} M to 3.2×10^{-4} M with an estimated correlation coefficient (R^2) of 0.9997 in the linear part of the response curve. For the SDS anion, the linear concentration ranged from 5.9×10^{-7} M to 4.1×10^{-3} M with an R^2 of 0.9998 in the linear part of the response curve. The limits of detection (LOD) were calculated according to IUPAC recommendations. [34] For DBS, the calculated LOD were 6.1×10^{-7} M and 5.5×10^{-7} M for SDS. The estimated slope values in the linear response region for DBS were 59.29 ± 0.5 mV/decade and for SDS anion 58.31 ± 0.4 mV/decade.

Table 2. Response characteristics of DODI–TPB surfactant sensor to anionic surfactants DBS and SDS in H_2O, given together with ±95% confidence limits.

Parameters	Anionic Surfactants	
	DBS	**SDS**
Slope (mV/decade)	59.3 ± 0.5	58.3 ± 0.4
Correlation coefficient (R^2)	0.9997	0.9998
Limit of detection (M)	7.1 ± 10^{-7}	6.8 ± 10^{-7}
Useful linear concentration range (M)	6.3×10^{-7} to 3.2×10^{-4}	5.9×10^{-7} to 4.1×10^{-3}

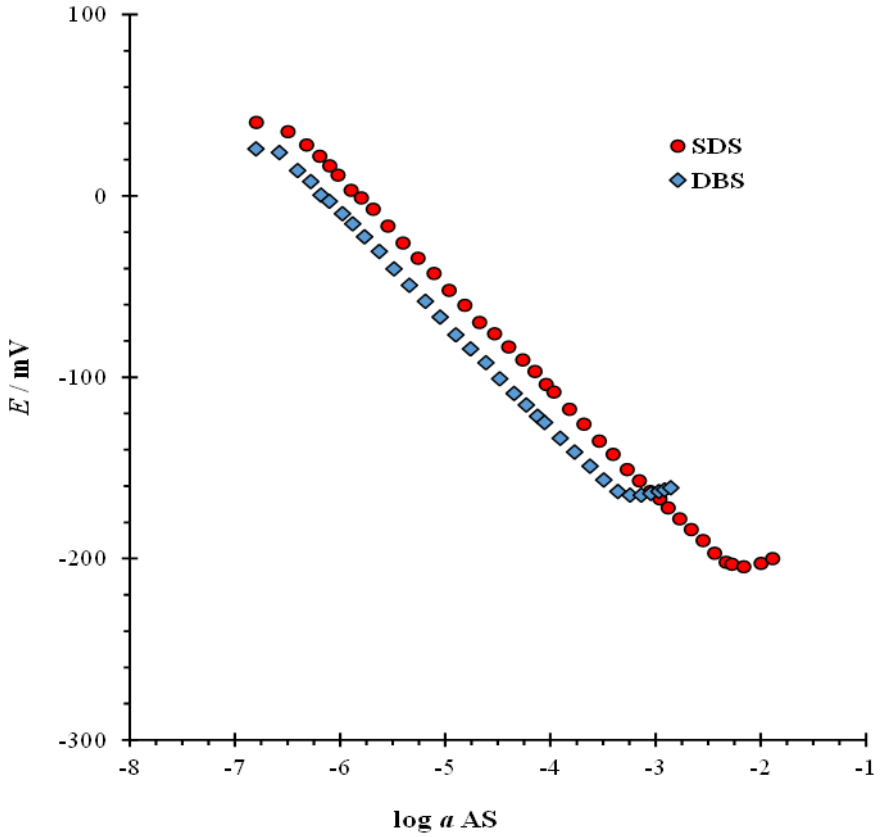

Figure 2. Direct potentiometric response characteristics of DODI–TPB surfactant sensor to anionic surfactants SDS and DBS in H_2O at a wide concentration range, with mean values at ±95% confidence limits.

3.3.2. Selectivity and pH

An interference study was performed to investigate the influence of some common organic and inorganic anions (present in products or waters and wastewaters) on the response characteristics of the DODI–TPB surfactant sensor in the presence of an anionic surfactant SDS in the broad concentration range from 5×10^{-6} to 5×10^{-3} M. The selected interfering anion concentration was 0.01 M. To calculate the selectivity coefficient, a fixed interference method [34] was applied. The selectivity was tested to observe the ability of the sensor to discriminate certain anions in the presence of interfering ions. The results of the calculated selectivity coefficient ($logK^{pot.}_{An^-_i}$) for different inorganic and organic interfering sodium salts are presented in Table 3. The DODI–TPB surfactant sensor showed good selectivity toward SDS in the presence of common interfering anions.

The response of the DODI–TPB surfactant sensor to SDS (0.5 mM) was tested in the range of pH 2 to 13 and is presented in Figure 3. The measured electromotive force was stable in the pH range from 2 to 9, and this pH region could be used in further investigations. At pH 10 to 13, the DODI–TPB surfactant sensor showed higher fluctuation in the signal change, and this region was not suitable for measurements. This likely comes as a result of the fact that both sensor components lack notably acidic/basic sites [35], which is why lowering the pH conditions exerts only a moderate effect, while a significant increase in the latter possibly disintegrates TBP^- due to the introduced OH^- anions that either compete with phenyl ligands for the boron coordination or help with the hydrolysis of either component.

Table 3. Calculated selectivity coefficient ($logK^{pot.}_{An_i^-}$) for different inorganic and organic interfering sodium salts (10 mM) for SDS response with the DODI–TPB surfactant sensor for SDS.

Anion	$logK^{pot.}_{An_i^-}$
Acetate	−4.27
Borate	−4.75
Benzoate	−4.35
Bromide	−4.00
Chloride	−3.92
Carbonate	−3.92
Dihydrogenphophate	−3.92
EDTA	−3.92
Hydrogen sulfate	−3.30
Nitrate	−3.43
Sulfate	−3.48
Toluensulfonate	−3.93

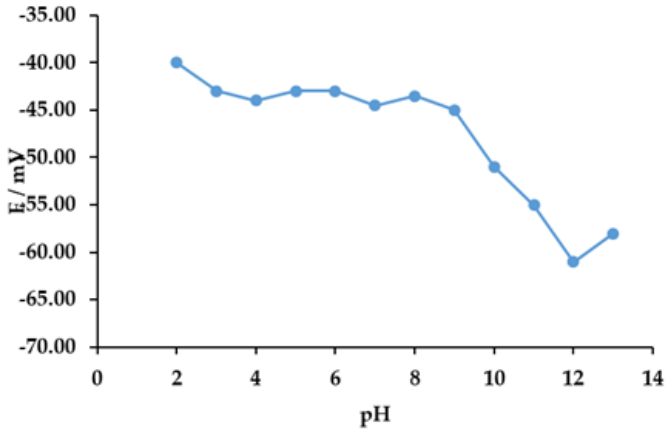

Figure 3. The response characteristics of DODI–TPB surfactant sensor towards SDS (0.5 mM) in deionized water at different pH levels.

3.4. Potentiometric Titrations

3.4.1. Titration of DBS with Selected Cationic Surfactants

Hyamine 1622, CTAB, CPC, and DMIC were used for the potentiometric titrations of DBS (4 mM) with selected cationic surfactants of analytical grade (4 mM). Titration conditions were the same for all measurements and the DODI–TPB surfactant sensor was used as the endpoint indicator. Potentiometric titration curves are shown in Figure 4. All titration curves had a sigmoidal shape with a well-defined signal change in the endpoint region. The DODI–TPB surfactant sensor showed the best signal change in the titrations with DMIC, where the signal change was 382.5 ± 2.4 mV. The signal change for CPC was 350.4 ± 3.1 mV, for CTAB 335.6 ± 1.9 mV, while the lowest signal change was obtained for Hyamine 1622, at 316.6 ± 3.2 mV. From the titration curves, the corresponding first derivatives were calculated ($\Delta E/\Delta V$) and included in Figure 4. Analogous to the titration curves data, the first derivative values for DMIC showed the highest change in the endpoint, 79.4 mV/mL, with a sharp peak. The first derivative values for the other three cationic surfactants, CPC, CTAB, and Hyamine1622, were 77.7, 77.3, and 62.1 mV/mL, respectively, with well-defined peaks. The falling properties of the cationic titrants for potentiometric titrations of DBS using the DODI–TPB surfactant sensor as the endpoint indicator were DMIC > CPC > CTAB > Hyamine 1622. All the studied cationic surfactants were suitable for DBS detection using the DODI–TPB surfactant sensor.

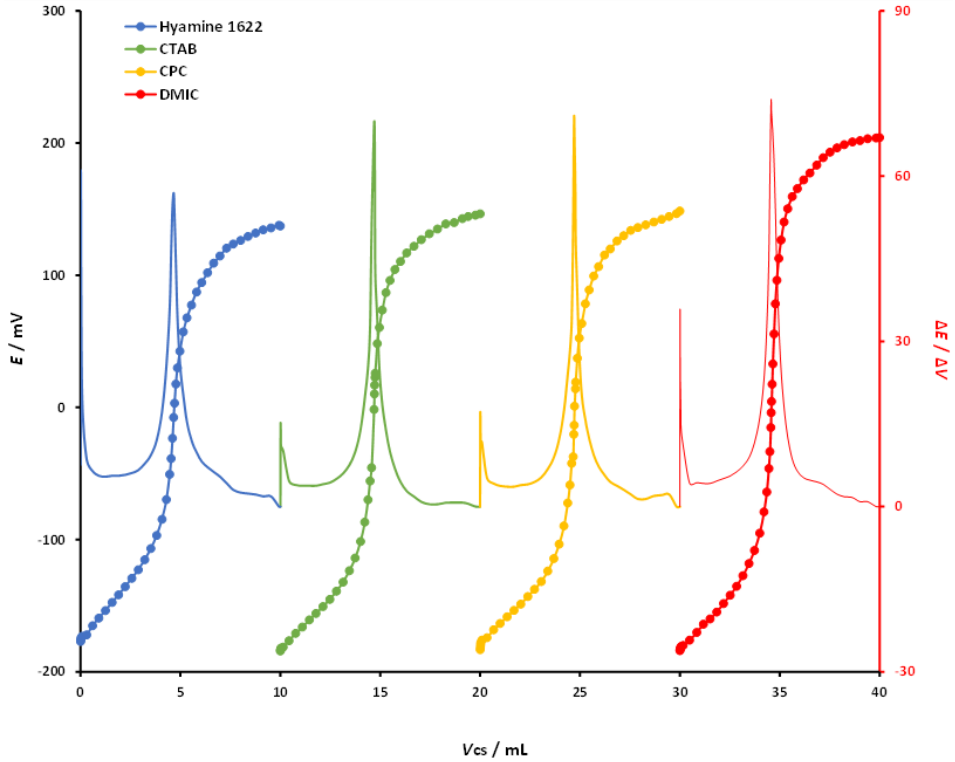

Figure 4. Potentiometric titration curves, and first derivatives, of DBS (0.4 mM) with four different cationic surfactants (0.4 mM) used as a titrant: Hyamine 1622, CTAB, CPC, and DMIC. The titration curves and their first derivatives were rearranged for the sake of clarity.

3.4.2. Titration of SDS with Selected Cationic Surfactants

For the potentiometric titrations of SDS, the same approach was used as for DBS. Hyamine 1622, CTAB, CPC, and DMIC were used for the potentiometric titrations of SDS (4 mM) with selected cationic surfactants of analytical grade (4 mM). Titration conditions were the same for all measurements, and the DODI–TPB surfactant sensor was used as the endpoint indicator. Potentiometric titration curves are shown in Figure 5. All titration curves had a sigmoidal shape with well-defined signal changes in the area of the endpoint. The DODI–TPB surfactant sensor showed the best signal change in the titrations with DMIC where the signal change was 376.5 ± 3.8 mV. The signal change for CPC was 319.3 ± 3.7 mV, for CTAB 303.9 ± 2.5 mV, while the lowest signal change was obtained for Hyamine 1622 with 272.4 ± 3.1 mV. From the titration curves, the corresponding first derivatives were calculated ($\Delta E/\Delta V$) and included in Figure 5. Analogous to the titration curve data, the first derivative values for DMIC showed the largest change in the endpoint, 79.6 mV/mL, with a sharp peak. The first derivative values for the three other cationic surfactants, CPC, CTAB, and Hyamine1622, were 75.7, 75.4, and 53.5 mV/mL, respectively, with well-defined peaks. The falling properties of the cationic titrants for potentiometric titrations of DBS using the DODI–TPB surfactant sensor as an endpoint indicator were DMIC > CPC > CTAB > Hyamine 1622. All of the studied cationic surfactants were suitable for SDS detection with the DODI–TPB surfactant sensor.

The standard addition of SDS and DBS at two concentration levels (0.1 and 0.01 mM) was used to estimate the accuracy of the DODI–TPB surfactant sensor. Selected cationic surfactants (Hyamine 1622, CTAB, CPC, and DMIC) were used as titrants. The measured and found concentrations of DBS and SDS, as well as the corresponding recoveries, are listed in Table 4. The recoveries for titrations of DBS ranged from 97.3 to 102.0%, with the best recoveries for DMIC being 99.3% (for 0.1 mM) and 99.7% (for 0.01 mM). The recoveries for the titrations of SDS ranged from 98.1 to 99.8%, with the best recovery for DMIC being 99.7% (for 0.1 mM) and 99.6% (for 0.01 mM). The proposed DODI–TPB surfactant sensor showed good accuracy against the studied anionic surfactants.

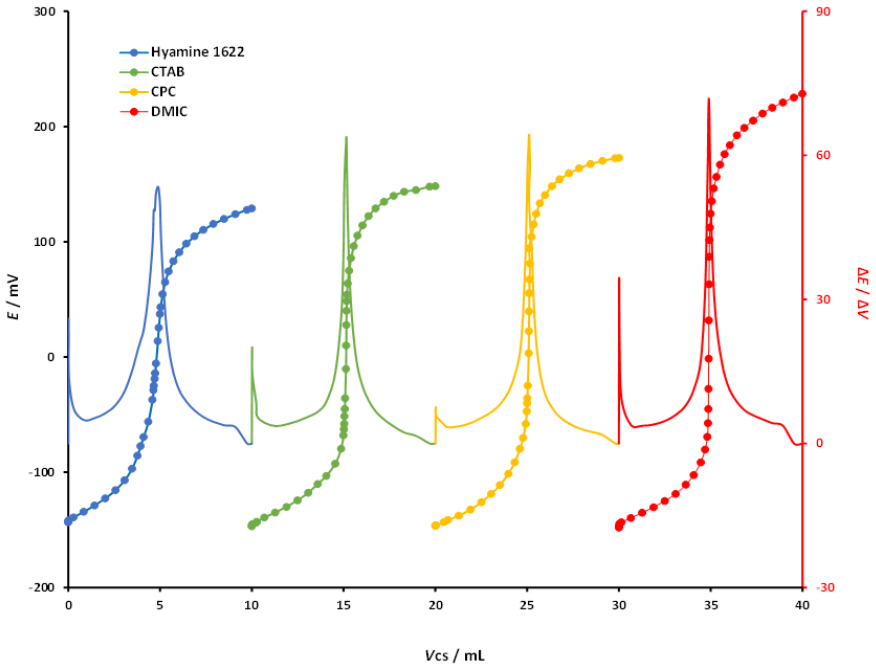

Figure 5. Potentiometric titration curves, and first derivatives, of SDS (0.4 mM) with four different cationic surfactants (0.4 mM) used as a titrant: Hyamine 1622, CTAB, CPC, and DMIC. The titration curves and their first derivatives were rearranged for the sake of clarity.

Table 4. Potentiometric titration results of SDS and DBS anionic surfactants with selected cationic surfactants (4 mM) as a titrant and the DODI–TPB surfactant sensor as an endpoint indicator.

		Analyte					
		DBS			SDS		
		Taken (mM)	Found (mM)	Recovery (%)	Taken (mM)	Found (mM)	Recovery (%)
Titrant	CTAB	0.1	0.0973	97.3	0.1	0.0989	98.9
		0.01	0.00102	102.0	0.01	0.00981	98.1
	Hyamine 1622	0.1	0.0972	97.2	0.1	0.0988	98.8
		0.01	0.00975	97.5	0.01	0.00989	98.9
	CPC	0.1	0.0993	99.3	0.1	0.0991	99.1
		0.01	0.00985	98.5	0.01	0.00987	98.9
	DMIC	0.1	0.0993	99.3	0.1	0.0998	99.7
		0.01	0.00997	99.7	0.01	0.00996	99.6

3.4.3. Titrations of Commercial Samples

The DODI–TPB surfactant sensor was used as an endpoint indicator in potentiometric titration of 12 commercial products containing anionic surfactants. These products were detergents intentionally divided into three groups: powder, liquid gel, and hand wash, to cover all potential product types. They were all declared to contain anionic surfactants. An appropriate concentration of CPC was used as a titrant. The studies with CPC showed good analytical properties, just below those of DMIC, but CPC was selected because the price of DMIC is much higher. Five independent titrations were performed for each detergent sample (Table 5). Hand detergents were found to have the highest levels of anionic surfactants ranging from 14.89 to 15.98%. Powder detergent samples contained 4.25 to 6.01% of anionic surfactants, while gel liquid detergents contained the lowest amounts of anionic surfactants, ranging from 2.11 to 3.21%. The data were compared with the previously published ISE DMI–TPB surfactant sensor [13] and a two-phase titration referent method [8], which revealed good agreement between all three methods.

Table 5. Potentiometric titration results of detergent commercial products with the DODI–TPB surfactant sensor as an endpoint indicator and CPC as a titrant, compared with the ISE surfactant sensor and a referent two-phase titration method.

Detergent Sample		% Anionic Surfactant		
		DODI–TPB	DMI–TPB [13]	Two-Phase Titration [8]
Solid/powder	Sample 1	4.25 ± 0.08	4.21	4.71
	Sample 2	5.21 ± 0.09	5.22	5.01
	Sample 3	5.66 ± 0.07	5.61	5.51
	Sample 4	6.01 ± 0.09	6.09	6.11
Liquid/gel	Sample 5	2.11 ± 0.07	2.15	2.27
	Sample 6	2.45 ± 0.11	2.41	2.85
	Sample 7	2.25 ± 0.09	2.26	2.41
	Sample 8	3.21 ± 0.09	3.27	3.28
Handwashing	Sample 9	15.22 ± 0.11	15.21	15.32
	Sample 10	14.89 ± 0.09	14.85	15.07
	Sample 11	15.42 ± 0.08	15.48	15.55
	Sample 12	15.98 ± 0.12	15.99	16.12

4. Conclusions

The new procedure for the direct synthesis of the 1,3-dioctadecyl-1*H*-imidazol-3-ium tetraphenylborate (DODI–TPB) ionophore was successfully applied. The DODI–TPB ionophore was characterized and confirmed by NMR, ATR FT-IR, LC–MS, and elemental analysis.

A computational analysis confirmed the feasibility of the DODI–TPB complex formation in solution and elucidated a range of C–H···π interactions among flexible C-18 alkyl chains in $DODI^+$ and phenyl groups in TPB^- as dominant for their recognition in solution. The calculated MM-PBSA binding affinity among components of $\Delta G_{BIND} = -5.0$ kcal mol^{-1} appears optimal, as it efficiently combines the ionophore stability with its ability to exchange anions in solution, thereby allowing for favorable analytic and sensing responses.

The DODI–TPB ionophore was used to fabricate the PVC-based liquid membrane-type potentiometric surfactant sensor for anionic surfactants. The DODI–TPB surfactant sensor exhibited good response characteristics, a wide linear response range (5.9×10^{-7}–4.1×10^{-3} M for SDS), a low detection limit (6.8×10^{-7} M for SDS), a Nernstian slope, high selectivity toward interfering anions, high accuracy (98.1–99.8% for SDS), and a wide operational pH range (2–9). Both anionic surfactants, DBS and SDS, were successfully titrated with four cationic surfactants, resulting in sigmoid curves with high potential changes (up to 382.5 mV), well-defined inflexions, and sharp endpoint peaks for the first derivatives. The DODI–TPB surfactant sensor was successfully used to quantify anionic surfactants in 12 commercially available detergents (powder, hand wash, and liquid gel detergents). The results show good agreement with the ISE surfactant sensor and the two-phase titration method. The DODI–TPB surfactant sensor could be used in quality control in the industry. Even though the sensor showed high stability and a broad response range, the sensor seems to be more suitable to observe surfactant concentrations in wastewaters than lakes and rivers. Further investigations will be conducted using the DODI–TPB surfactant sensor to quantify anionic surfactants in water and wastewater.

Supplementary Materials: The following supporting information can be downloaded at: https://www.mdpi.com/article/10.3390/chemosensors10120523/s1, Figure S1: 1H NMR (400 MHz; CDCl3) of 1,3-dioctadecyl-1H-imidazol-3-ium tetraphenylborate (2); Figure S2: 13C NMR (100.613 MHz; CDCl3) of 1,3-dioctadecyl-1H-imidazol-3-ium tetraphenylborate (2); Figure S3: ATR-FTIR spectra of powder 1,3-dioctadecyl-1H-imidazol-3-ium tetraphenylborate (2); Figure S4: RMSD graphs during the molecular dynamics simulation in the aqueous solution; Figure S5: Time dependence of the

distance between the boron atom in TPB− and the nitrogen atoms in DODI+ during the molecular dynamics simulation; Figure S6: Charge distribution within the DODI+ cation and the TPB− anion.

Author Contributions: Conceptualization, M.J. and N.S.; Methodology, M.J., N.S.; D.M.-Č. and R.V. (Robert Vianello); Formal Analysis, D.M.-Č., N.S., D.M., L.H., V.V. and M.J.; Investigation, M.J., N.S., D.M.-Č. and L.H.; Resources, M.J., N.S., B.Š., R.V. (Robert Vianello) and B.Đ.; Data Curation, N.S., D.M., D.M.-Č., L.H., V.V., B.D.V., R.V. (Raffaele Velotta) and M.J.; Writing—Original Draft Preparation, N.S., M.J., D.M.-Č., B.Š. and R.V. (Robert Vianello); Writing—Review and Editing, N.S., D.M., R.V. (Robert Vianello) and M.J.; Visualization, L.H., B.Š., B.D.V., R.V. (Raffaele Velotta) and B.Đ.; Supervision, M.J., N.S. and R.V. (Robert Vianello); Project Administration, M.J. and N.S. All authors have read and agreed to the published version of the manuscript.

Funding: Croatian Science Foundation, projects IP-2019-04-8846, IP-2020-02-8090, and DOK-2020-01-3482.

Institutional Review Board Statement: Not applicable.

Informed Consent Statement: Not applicable.

Data Availability Statement: The data presented in this study are available in the Supplementary Materials.

Acknowledgments: N.S., B.Š. and M.J. would like to thank the EuChemS Sample Preparation Task Force and Network. N.S., B.D.V. and R.V. would like to thank the COST Action PortASAP—European network for the promotion of portable, affordable and simple analytical platforms. D.M. would like to thank to Croatian Science Foundation for funding the research project IP-2019-04-8846 and the University of Rijeka for funding the research grant UNIRI-prirod-18-102. L.H. and R.V. (Robert Vianello) would like to thank the Croatian Science Foundation for a financial support (IP-2020-02-8090) and the Zagreb University Computing Centre (SRCE) for granting computational resources on the ISABELLA cluster. L.H. wishes to thank the Croatian Science Foundation for a doctoral stipend through the Career Development Project for Young Researchers (DOK-2020-01-3482).

Conflicts of Interest: The authors declare no conflict of interest.

References

1. Sakač, N.; Marković, D.; Šarkanj, B.; Madunić-Čačić, D.; Hajdek, K.; Smoljan, B.; Jozanović, M. Direct Potentiometric Study of Cationic and Nonionic Surfactants in Disinfectants and Personal Care Products by New Surfactant Sensor Based on 1,3-Dihexadecyl−1H-Benzo[d]Imidazol−3-Ium. *Molecules* **2021**, *26*, 1366. [CrossRef] [PubMed]
2. Fizer, O.; Filep, M.; Pantyo, V.; Elvira, D.; Fizer, M. Structural Study and Antibacterial Activity of Cetylpyridinium Dodecyl Sulfate Ion Pair. *Biointerface Res. Appl. Chem.* **2022**, *12*, 3501–3512. [CrossRef]
3. Jozanović, M.; Sakač, N.; Karnaš, M.; Medvidović-Kosanović, M. Potentiometric Sensors for the Determination of Anionic Surfactants—A Review. *Crit. Rev. Anal. Chem.* **2019**, *51*, 115–137. [CrossRef] [PubMed]
4. Research and Markets Global Surfactants Market (2019 to 2025)—Drivers, Restraints, Opportunities and Challenges. Available online: https://www.prnewswire.com/news-releases/global-surfactants-market-2019-to-2025---drivers-restraints-opportunities-and-challenges-301086922.html (accessed on 13 November 2022).
5. *Global Anionic Surfactants Market—Industry Trends and Forecast to 2027*; Data Bridge Market Research: Pune, India, 2020.
6. Effendy, I.; Maibach, H.I. Surfactants and Experimental Irritant Contact Dermatitis. *Contact Dermat.* **1995**, *33*, 217–225. [CrossRef] [PubMed]
7. Venhuis, S.H.; Mehrvar, M. Health Effects, Environmental Impacts, and Photochemical Degradation of Selected Surfactants in Water. *Int. J. Photoenergy* **2004**, *6*, 115–125. [CrossRef]
8. *ISO 2271*; International Organization for Standardization Surface Active Agents, Detergents, Determination of Anionic-Active Matter by Manual or Mechanical Direct Two-Phase Titration Procedure. ISO: Geneva, Switzerland, 1989.
9. Dimeski, G.; Badrick, T.; John, A.S. Ion Selective Electrodes (ISEs) and Interferences—A Review. *Clin. Chim. Acta* **2010**, *411*, 309–317. [CrossRef]
10. Fizer, M.; Fizer, O.; Sidey, V.; Mariychuk, R.; Studenyak, Y. Experimental and Theoretical Study on Cetylpyridinium Dipicrylamide—A Promising Ion-Exchanger for Cetylpyridinium Selective Electrodes. *J. Mol. Struct.* **2019**, *1187*, 77–85. [CrossRef]
11. Fizer, O.; Fizer, M.; Sidey, V.; Studenyak, Y. Predicting the End Point Potential Break Values: A Case of Potentiometric Titration of Lipophilic Anions with Cetylpyridinium Chloride. *Microchem. J.* **2021**, *160*, 105758. [CrossRef]
12. Najafi, M.; Maleki, L.; Rafati, A.A. Novel Surfactant Selective Electrochemical Sensors Based on Single Walled Carbon Nanotubes. *J. Mol. Liq.* **2011**, *159*, 226–229. [CrossRef]

13. Sakač, N.; Karnaš, M.; Jozanović, M.; Medvidović-Kosanović, M.; Martinez, S.; Macan, J.; Sak-Bosnar, M. Determination of Anionic Surfactants in Real Samples Using a Low-Cost and High Sensitive Solid Contact Surfactant Sensor with MWCNTs as the Ion-to-Electron Transducer. *Anal. Methods* **2017**, *9*, 2305–2314. [CrossRef]
14. Seguí, M.J.; Lizondo-Sabater, J.; Martínez-Máñez, R.; Pardo, T.; Sancenón, F.; Soto, J. Ion-Selective Electrodes for Anionic Surfactants Using a New Aza-Oxa-Cycloalkane as Active Ionophore. *Anal. Chim. Acta* **2004**, *525*, 83–90. [CrossRef]
15. Samardžić, M.; Budetić, M.; Széchenyi, A.; Marković, D.; Živković, P.; Šarkanj, B.; Jozanović, M. The Novel Anionic Surfactant Selective Sensors Based on Newly Synthesized Quaternary Ammonium Salts as Ionophores. *Sens. Actuators B Chem.* **2021**, *343*, 130103. [CrossRef]
16. Kovács, B.; Csóka, B.; Nagy, G.; Ivaska, A. All-solid-state surfactant sensing electrode using conductive polymer as internal electric contact. *Anal. Chim. Acta* **2001**, *437*, 67–76. [CrossRef]
17. Matysik, S.; Matysik, F.M.; Einicke, W.D. A disposable electrode based on zeolite-polymer membranes for potentiometric titrations of ionic surfactants. *Sens. Actuators B Chem.* **2002**, *85*, 104–108. [CrossRef]
18. Madunič-Čačić, D.; Sak-Bosnar, M.; Matešić-Puač, R. A New Anionic Surfactant-Sensitive Potentiometric Sensor with a Highly Lipophilic Electroactive Material. *Int. J. Electrochem. Sci.* **2011**, *6*, 240–253.
19. Sakač, N.; Madunić-Čačić, D.; Karnaš, M.; Đurin, B.; Kovač, I.; Jozanović, M. The Influence of Plasticizers on the Response Characteristics of the Surfactant Sensor for Cationic Surfactant Determination in Disinfectants and Antiseptics. *Sensors* **2021**, *21*, 3535. [CrossRef]
20. Olkowska, E.; Polkowska, Z.; Namieśnik, J. Analytical Procedures for the Determination of Surfactants in Environmental Samples. *Talanta* **2012**, *88*, 1–13. [CrossRef]
21. Pires, A.R.; Araújo, A.N.; Montenegro, M.C.B.S.M.; Chocholous, P.; Solich, P. New Ionophores for Vitamin B1 and Vitamin B6 Potentiometric Sensors for Multivitaminic Control. *J. Pharm. Biomed. Anal.* **2008**, *46*, 683–691. [CrossRef]
22. Mahajan, R.K.; Shaheen, A. Effect of Various Additives on the Performance of a Newly Developed PVC Based Potentiometric Sensor for Anionic Surfactants. *J. Colloid Interface Sci.* **2008**, *326*, 191–195. [CrossRef]
23. Devi, S.; Chattopadhyaya, M.C. Determination of Sodium Dodecyl Sulfate in Toothpastes by a PVC Matrix Membrane Sensor. *J. Surfactants Deterg.* **2013**, *16*, 391–396. [CrossRef]
24. Issa, Y.M.; Mohamed, S.H.; Baset, M.A. El Chemically Modified Carbon Paste and Membrane Sensors for the Determination of Benzethonium Chloride and Some Anionic Surfactants (SLES, SDS, and LABSA): Characterization Using SEM and AFM. *Talanta* **2016**, *155*, 158–167. [CrossRef] [PubMed]
25. Arooj, M.; Arrigan, D.W.M.; Mancera, R.L. Characterization of Protein-Facilitated Ion-Transfer Mechanism at a Polarized Aqueous/Organic Interface. *J. Phys. Chem. B* **2019**, *123*, 7436–7444. [CrossRef] [PubMed]
26. Case, D.A.; Betz, R.M.; Cerutti, D.S.; Cheatham, T.E., III; Darden, T.A.; Duke, R.E.; Giese, T.J.; Gohlke, H.; Goetz, A.W.; Homeyer, N.; et al. *AMBER 2016*; University of California: San Francisco, CA, USA, 2016.
27. Genheden, S.; Ryde, U. The MM/PBSA and MM/GBSA Methods to Estimate Ligand-Binding Affinities. *Expert Opin. Drug Discov.* **2015**, *10*, 449–461. [CrossRef] [PubMed]
28. Hou, T.; Wang, J.; Li, Y.; Wang, W. Assessing the Performance of the MM/PBSA and MM/GBSA Methods. 1. The Accuracy of Binding Free Energy Calculations Based on Molecular Dynamics Simulations. *J. Chem. Inf. Model.* **2011**, *51*, 69–82. [CrossRef] [PubMed]
29. Sakač, N.; Madunić-Čačić, D.; Marković, D.; Hok, L.; Vianello, R.; Šarkanj, B.; Đurin, B.; Hajdek, K.; Smoljan, B.; Milardović, S.; et al. Potentiometric Surfactant Sensor Based on 1,3-Dihexadecyl-1H-Benzo[d]Imidazol-3-Ium for Anionic Surfactants in Detergents and Household Care Products. *Molecules* **2021**, *26*, 3627. [CrossRef]
30. Hok, L.; Mavri, J.; Vianello, R. The Effect of Deuteration on the H2 Receptor Histamine Binding Profile: A Computational Insight into Modified Hydrogen Bonding Interactions. *Molecules* **2020**, *25*, 6017. [CrossRef]
31. Hok, L.; Rimac, H.; Mavri, J.; Vianello, R. COVID-19 Infection and Neurodegeneration: Computational Evidence for Interactions between the SARS-CoV-2 Spike Protein and Monoamine Oxidase Enzymes. *Comput. Struct. Biotechnol. J.* **2022**, *20*, 1254–1263. [CrossRef]
32. Galović, O.; Samardžić, M.; Petrušić, S.; Sak-Bosnar, M. A New Sensing Material for the Potentiometric Determination of Anionic Surfactants in Commercial Products. *Int. J. Electrochem. Sci.* **2014**, *9*, 3802–3818.
33. Mao, C.; Robinson, K.J.; Yuan, D.; Bakker, E. Ion–ionophore interactions in polymeric membranes studied by thin layer voltammetry. *Sens. Actuators B Chem.* **2022**, *358*, 131428. [CrossRef]
34. Buck, R.P.; Lindner, E. Recomendations for Nomenclature of Ion-Selective Electrodes (IUPAC Recommendations 1994). *Pure Appl. Chem.* **1994**, *66*, 2527–2536. [CrossRef]
35. Tshepelevitsh, S.; Kütt, A.; Lõkov, M.; Kaljurand, I.; Saame, J.; Heering, A.; Plieger, P.G.; Vianello, R.; Leito, I. On the Basicity of Organic Bases in Different Media. *Eur. J. Org. Chem.* **2019**, *2019*, 6735–6748. [CrossRef]